

# Modification of GaAs/AlGaAs growth-interrupted interfaces through changes in ambient conditions during growth

R. F. Kopf, E. F. Schubert, T. D. Harris, R. S. Becker, and G. H. Gilmer  
*AT&T Bell Laboratories, Murray Hill, New Jersey 07974*

(Received 5 April 1993; accepted for publication 14 June 1993)

The effect of the ambient conditions in the growth chamber of the molecular beam epitaxy machine during the growth of GaAs/Al<sub>0.35</sub>Ga<sub>0.65</sub>As structures was investigated. Both growth-interrupted (120 s at each heterointerface) and uninterrupted surfaces and interfaces were evaluated using a growth temperature of 580 °C. Two ambient conditions were studied: (a)  $\sim 1 \times 10^{-10}$  Torr O<sub>2</sub>; and (b) ultrahigh vacuum (UHV,  $\sim 5 \times 10^{-11}$  Torr, with no intentional introduction of contaminants). A striking difference was observed in both the 1.7 K photoluminescence (PL) spectra of single quantum well (SQW) structures and UHV scanning tunneling microscopy (STM) of surfaces, which were grown under ambient condition (a) as opposed to (b). When consecutive growth-interrupted SQW samples were grown with different well widths (25 and 28 Å) under condition (a), the emission energy splitting into several peaks was observed, indicating discrete thicknesses of the well. However, the peak energies shifted as the laser spot was scanned across each sample. Additionally, the peak energy shifted from sample to sample for the same nominal well width. On the other hand, when SQW samples were grown under condition (b), no variation in the emission energy was observed as the laser was scanned across the sample, or from sample to sample for a given well width. Furthermore, the PL observations are supported by UHV-STM results. UHV-STM images indicated a very rough surface with large islands containing small terraces on top (a bimodal distribution) for condition (a). Conversely, when samples were grown under condition (b), only large islands were observed. For growth interrupted GaAs surfaces, 400 Å × 600 Å islands were observed, and for Al<sub>0.35</sub>Ga<sub>0.65</sub>As, they were 150 Å × 400 Å, with a one-monolayer step in between islands. These data are consistent with abrupt interfaces with only a single-mode distribution for growth-interrupted surfaces. On the other hand, UHV-STM images of uninterrupted GaAs surfaces grown under condition (b) showed islands that were 40–60 Å across. Photoluminescence spectra of a similarly grown SQW sample showed only a single broad emission line, consistent with an interface configuration of many steps which are smaller than the exciton diameter. The results show that interface roughness is sensitive to background O<sub>2</sub>.

## I. INTRODUCTION

Molecular beam epitaxy (MBE) is routinely used to fabricate high-quality GaAs/Al<sub>x</sub>Ga<sub>1-x</sub>As electronic and optoelectronic structures, since it offers precise control of the thickness, doping, and composition over macroscopic distances (> 3 in.). However, the microscopic structure of GaAs/Al<sub>x</sub>Ga<sub>1-x</sub>As heterointerfaces remains an intense subject of research. Growth interruption at these heterointerfaces changes their structural characteristics considerably. Structural changes are inferred from the splitting of the single, broadened 1.7 K photoluminescence (PL) emission line observed in single quantum well (SQW) samples grown without interruption into two or more sharp lines for growth-interrupted samples.<sup>1-4</sup> Both the emission line energy and the energy splitting of the emission lines are constant over macroscopic distances ( $\sim 2$  in.).<sup>3</sup> These growth-interrupted interfaces are stable with time, and no changes in optical or structural characteristics have been reported.

In order to discuss interface configurations, we must consider the size of the "optical probe" in the PL measurements. Since radiative recombination in semiconductor quantum well samples is excitonic in nature, we use the

hydrogen model to estimate the Bohr radius of excitons in quantum wells, which is the spatial lateral resolution of the optical probe. The three-dimensional (3D) exciton Bohr radius is given by

$$r_{\text{exciton}}^{3\text{D}} = \left( \frac{\epsilon}{\epsilon_0} \frac{m_0}{m_r^*} \right) 0.53 \text{ \AA},$$

where  $\epsilon$  is the permittivity of GaAs and  $m_r^*$  is the reduced mass of the electron-heavy-hole pair. Using  $\epsilon/\epsilon_0 = 11.5$  (high frequency) and  $m_r^* = 0.0556m_0$ , we obtain  $r_{\text{exciton}} = 110 \text{ \AA}$ . However, the thickness of our single quantum well structures is only around 25 Å, much smaller than the 3D Bohr radius. Therefore, we must use the two-dimensional (2D) Bohr radius, which is, in the 2D limit, given by  $r_{\text{exciton}}^{2\text{D}} = \frac{1}{2} r_{\text{exciton}}^{3\text{D}} \cong 50 \text{ \AA}$ . Thus the size of our optical probe is on the order of the 2D exciton diameter ( $\sim 100 \text{ \AA}$ ), with a maximum sensitivity around 50 Å. That is, PL measurements are exceedingly sensitive to roughness on a 50 Å lateral scale, whereas any interface roughness on length scales  $\ll 50 \text{ \AA}$  (e.g., 5 Å) or  $\gg 50 \text{ \AA}$  (e.g., 500 Å) cannot be assessed by PL.

Keeping in mind the size of the optical probe, it is useful to define the following interface configurations. First

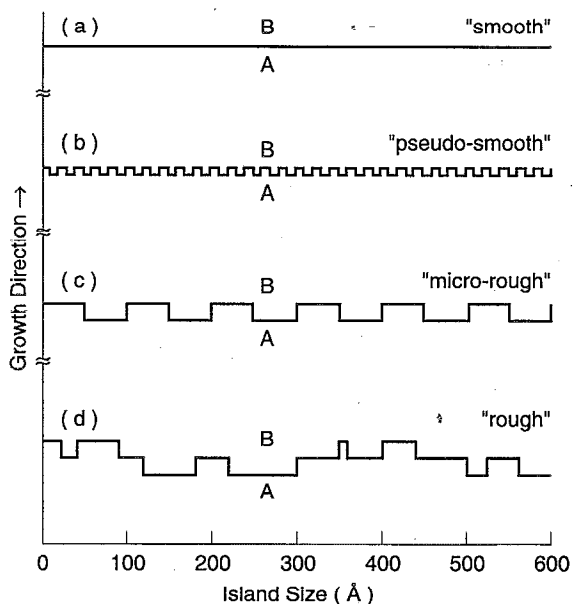


FIG. 1. Various interface configurations between two semiconductors, A and B: (a) smooth interface with no intermixing; (b) pseudosmooth interface with intermixing from diffusion or segregation; (c) microrough interface containing a small island structure, which was on A before B was deposited; and (d) rough interface where the interface position contains a large range of island sizes.

a smooth interface is obtained if a semiconductor B is grown on top of an atomically flat semiconductor A and no intermixing occurs. Second, a pseudosmooth interface is obtained if B is grown on top of A and intermixing (diffusion or segregation) occurs. Note that such intermixing processes are random events, which do not introduce roughness with a lateral correlation length. Third, a microrough interface contains significant roughness on a 50 Å lateral length scale. Such an interface can be the result of a small island structure ( $\sim 50$  Å) on semiconductor A, before B is grown on top of it. Finally, a rough interface has variations of the interface position with a large range of lateral correlation lengths (e.g., 5–500 Å). These four interface configurations are illustrated in Figs. 1(a) through 1(d), respectively.

Previously, we suggested interface configurations which would produce the PL results for growth-interrupted SWQ samples.<sup>3</sup> These interface configurations consist of one or two smooth or pseudosmooth interfaces. For illustrative purposes, a SQW sample with "smooth" interfaces is depicted in Fig. 2. The expected PL emission characteristics for monolayer splitting of the broad emission line into several lines are also shown. Both top and bottom interfaces are smooth and have large islands, which are greater than the 2D exciton diameter ( $\sim 100$  Å). However, if one interface is smooth, and the other has a distribution consisting of large islands ( $\sim 100$  Å), with much smaller islands ( $\sim 5$  Å) on top, the same PL emission characteristics would be obtained. For simplicity, these two models are referred to as "smooth" and "pseudo-smooth," respectively.<sup>1,3</sup> To differentiate between the two above interface configurations, multiple samples must be

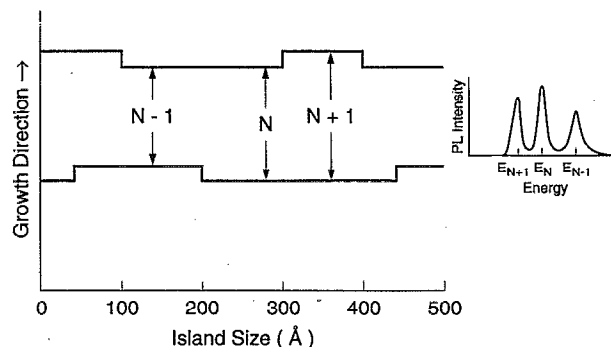


FIG. 2. Schematic illustration of a SQW sample with smooth interfaces, along with the expected PL emission characteristics.

studied,\* since the absolute emission energy should be a constant for a given interface configuration (well width, barrier height) with the smooth interface model, but not for the pseudosmooth model. The latter appears to be the case when studying SQW samples with GaAs wells and AlAs barriers,<sup>1,5</sup> although it is probably not when utilizing lower Al concentrations in the barriers.<sup>6</sup> In fact, reflection high-energy diffraction (RHEED) intensity recovery characteristics during a growth interruption indicate that the GaAs surface is the smoothest, the AlAs surface remains rough, and  $\text{Al}_x\text{Ga}_{1-x}\text{As}$  with  $0 < x < 1$  is somewhere in between, for a given growth temperature and V/III flux ratio.<sup>7,8</sup>

In this publication, we study the sample to sample variation of absolute PL emission energy for growth-interrupted SQW samples of  $\text{Al}_{0.35}\text{Ga}_{0.65}\text{As}/\text{GaAs}/\text{Al}_{0.35}\text{Ga}_{0.65}\text{As}$ , which were grown under different background vacuum conditions. We also report on UHV scanning tunneling microscopy (STM) images of surfaces which were prepared in an identical manner as the top and bottom interfaces of the SQW, except that they were capped with  $\sim 1000$  Å of  $\text{As}_4$ , prior to transfer to the STM. We particularly study the island sizes for both GaAs and  $\text{Al}_{0.35}\text{Ga}_{0.65}\text{As}$  surfaces. These surfaces are representative of the actual SQW interfaces, since molecular dynamics calculations show negligible interface mixing occurs at our growth temperature of 580 °C. However, we find that the distribution of island sizes is extremely sensitive to the ambient vacuum conditions during growth. UHV-STM images show that the presence of  $10^{-10}$  Torr  $\text{O}_2$  during growth results in a pseudosmooth or microrough island distribution for both GaAs and  $\text{Al}_{0.35}\text{Ga}_{0.65}\text{As}$  surfaces. The PL emission characteristics of SQW samples grown under this latter condition are consistent with both interfaces containing a microrough configuration, since the emission energies vary across each sample, as well as from sample to sample for a given well geometry.

## II. EXPERIMENTAL

Samples were grown in an Intevac Gen II MBE machine on 2 in., undoped, (100) GaAs substrates, at 580 °C,

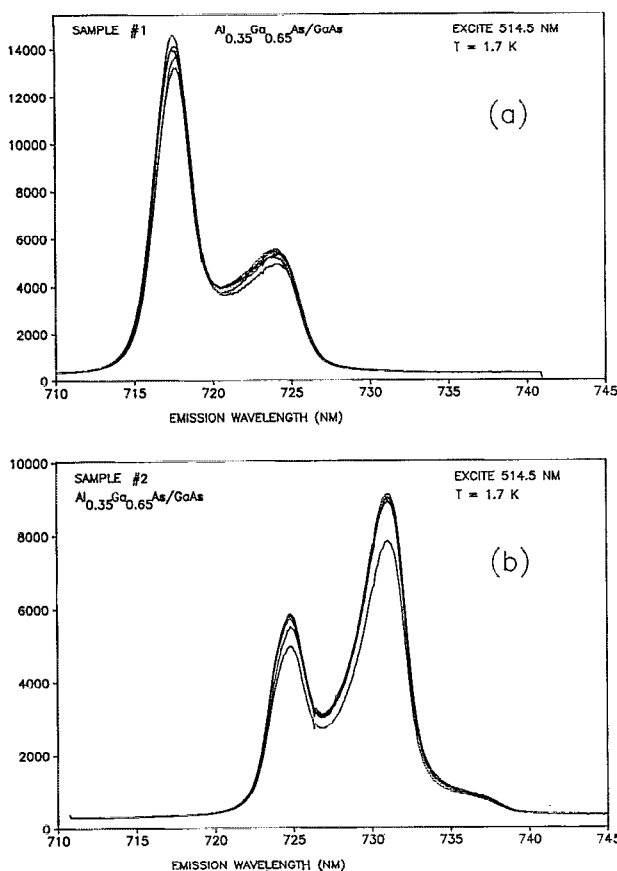


FIG. 3. PL emission spectra of growth-interrupted SQW samples grown under UHV conditions: sample 1, 25 Å well; sample 2, 28 Å well. The emission energies are constant as the laser is scanned across each sample, and from sample to sample for a given well width, consistent with both interfaces having islands larger than the exciton diameter.

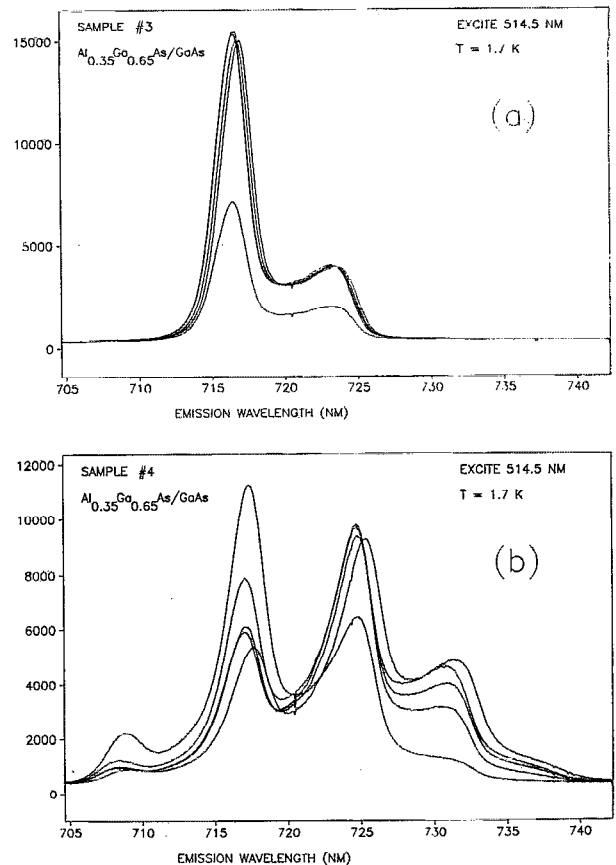


FIG. 4. PL emission spectra of growth-interrupted SQW samples grown in the presence of  $1 \times 10^{-10}$  Torr  $O_2$ : sample 3, 25 Å well; sample 4, 28 Å well. The emission energies vary as the laser is scanned across each sample, and from sample to sample, indicating that both of the interfaces have a pseudosmooth or microrough configuration.

with substrate rotation. For the SQW samples, the rotation speed was adjusted such that the sample was subjected to an integer number of revolutions during the growth of the well to ensure a uniform thickness across the wafer. The SQW structures consisted of a 5000 Å GaAs buffer layer, 1000 Å  $Al_{0.35}Ga_{0.65}As$  confining layers, either a 25 or 28 Å quantum well, and a 20 Å GaAs cap layer. A 120 s growth interruption was employed at each quantum well heterointerface. The GaAs and  $Al_{0.35}Ga_{0.65}As$  structures prepared for STM measurements were grown under the same conditions as the SQW samples, except that growth was terminated after either the bottom  $Al_{0.35}Ga_{0.65}As$  barrier layer or the 25 Å GaAs well layer. They were then annealed for 120 s under an  $As_4$  flux at the growth temperature. One of the STM samples with a GaAs top layer was grown without the 120 s anneal for comparison. 1000 Å of  $As_4$  was then deposited on them to prevent any surface oxidation during transfer in air to the UHV-STM. The  $As_4$  was sublimed at 365 °C in the UHV-STM just prior to measurements.

The GaAs growth rate was  $\sim 0.5 \mu\text{m/h}$ , and the AlAs growth rate was adjusted to obtain the desired Al mole fraction. Growth rates and compositions were determined using RHEED oscillations. The two ambient growth con-

ditions studied were UHV ( $\sim 5 \times 10^{-11}$  Torr, with no intentional introduction of impurities), and  $\sim 1 \times 10^{-10}$  Torr  $O_2$  (introduced through a leak valve). UHV-STM measurements were performed at a bias of +2 V and 50 pA. Photoluminescence measurements were performed at 1.6 K using the 5145 Å line of an  $Ar^+$  laser as the excitation source. Detection was with a Si charge-coupled device camera array, and peak energies were evaluated directly by a computer.

### III. RESULTS AND DISCUSSION

Quantum well samples discussed here were grown under high-quality UHV conditions and with  $1 \times 10^{-10}$  Torr  $O_2$  purposely leaked into the UHV recipient. We first discuss the PL results on the samples grown under UHV conditions. The low-temperature PL spectra of two SQW samples with well widths of 25 and 28 Å are shown in Figs. 3(a) and 3(b), respectively. Several PL spectra are overlaid in the figure to show that there is no change in emission energy across the sample. A clear splitting of the photoluminescence signal into three peaks is observed on both samples. The most striking feature of the two PL spectra shown in Fig. 3 is the coincidence of the peak energies of

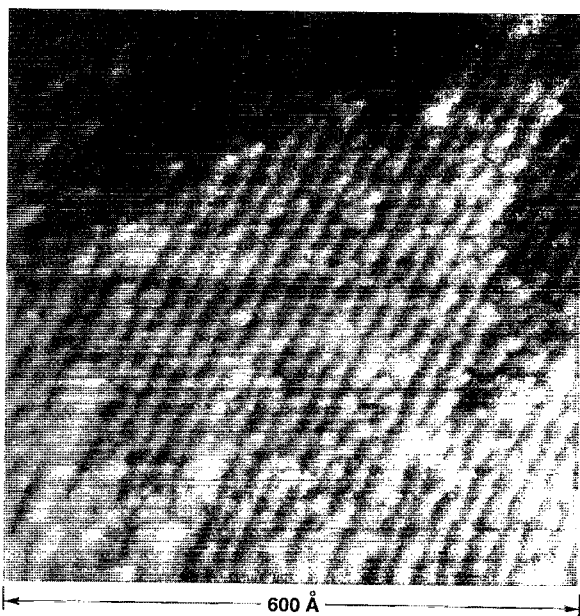


FIG. 5. UHV-STM image of a growth-interrupted GaAs surface showing one large island, about 600 Å in diameter.

the low-energy peak of the  $L_z=25$  Å sample and the high-energy peak of the  $L_x=28$  Å sample. That is, the emission energies of the PL spectra are “quantized” even if the well width is changed. A “quantization” of the peak energies is

fully consistent with smooth interfaces and a quantum well width which changes by one or a multiple integer of monolayers. The quantization is inconsistent with a microrough interface configuration. We also point out that the emission wavelengths were within 1 Å from sample to sample for a given well width, which is within the instrumental resolution, since baseline separation between the peaks was not achieved. This is consistent with the smooth interface model illustrated in Fig. 2.

Next, we discuss the low-temperature PL results obtained on samples subjected to  $1 \times 10^{-10}$  Torr  $O_2$ . The photoluminescence results are shown in Figs. 4(a) and 4(b). Several PL spectra taken within an area of  $1 \text{ cm}^2$  are overlaid in the figure to facilitate the comparison of peak energies. Figure 4 reveals that the peak energies vary as the exciting laser beam is moved across the sample. Furthermore, the PL spectra reveal that the peak energies are not “quantized” as is the case for the samples grown under high-quality UHV conditions. We therefore conclude that the samples shown in Fig. 4 are consistent with (partially) pseudosmooth or microrough interfaces. The PL spectra are inconsistent with smooth interfaces.

To investigate the possible interface configurations further, several samples were evaluated by UHV-STM. Images of growth-interrupted samples, which were grown under high-quality UHV conditions, were evaluated first. GaAs surfaces contained elongated islands, typically 400

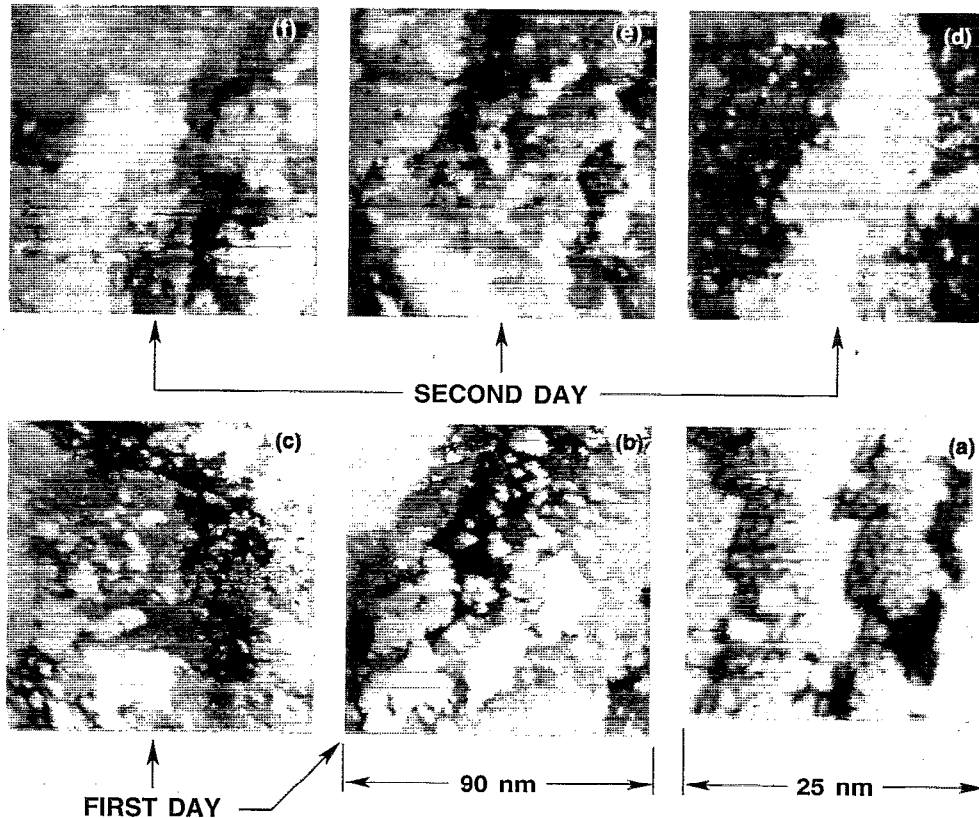


FIG. 6. UHV-STM image of a growth-interrupted  $Al_{0.35}Ga_{0.65}As$  surface showing large islands,  $150 \text{ Å} \times 400 \text{ Å}$  in size (a). This series of pictures also shows the AlGaAs surface oxidizing in the UHV-STM at  $1 \times 10^{-10}$  Torr over several hours [pictured from right to left (b) and (c)] and the following day [top pictures (d) through (f)].

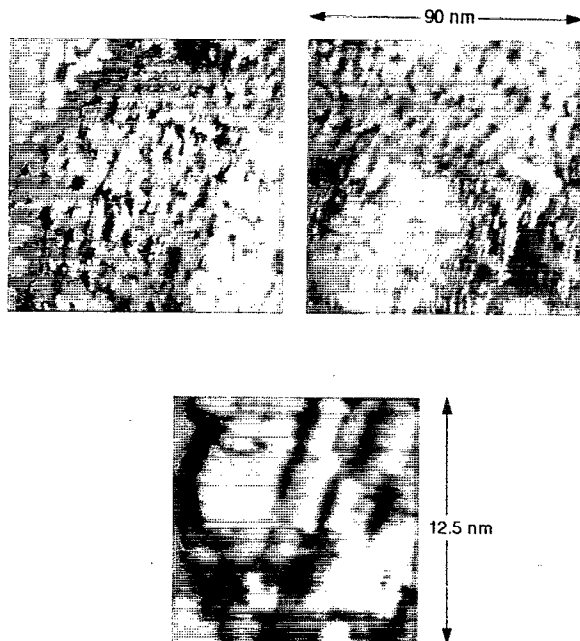


FIG. 7. UHV-STM image of an uninterrupted GaAs surface showing small islands, about 30 and 60 Å across.

Å × 600 Å, separated by single atomic steps (see Fig. 5). The  $\text{Al}_{0.35}\text{Ga}_{0.65}\text{As}$  islands shown in Fig. 6(a) are  $\sim 150$  Å × 400 Å, which is smaller than the GaAs islands, but still larger than the 2D exciton diameter. The smaller island size is attributed to a smaller Al surface diffusion coefficient as compared to Ga. A smaller surface diffusion coefficient is expected due to the higher Al—As bond strength as compared to the Ga—As bond strength. UHV-STM images of the Al containing layers had to be obtained within an hour of the As sublimation, since the sample oxidized in the UHV-STM chamber after 3–4 h. Figures 6(b) and 6(c) are UHV-STM images taken 3–4 h after the surface was exposed in the STM, and 6(d)–6(f) were taken the next day. The bright regions in these images are of Al containing oxides. This oxidation was unexpected, since the background pressure was  $\sim 10^{-10}$  Torr, with no leaks. No oxidation of the GaAs surfaces was observed even after several days in the UHV-STM. Uninterrupted GaAs surfaces were also evaluated to ensure that we were not altering the surface structure during sample transfer in air or during the As sublimation step. These images show elongated islands, about 30–60 Å in diameter, with a single atomic step in between (see Fig. 7).

On the other hand, UHV-STM images of growth-interrupted samples which were grown under  $1 \times 10^{-10}$  Torr  $\text{O}_2$  showed a drastically different surface configuration. Both GaAs and  $\text{Al}_{0.35}\text{Ga}_{0.65}\text{As}$  surfaces have a pseudosmooth or microrough island distribution, as shown in Figs. 8(a) and 8(b). This island size distribution is most likely due to  $\text{O}_2$  dissociation on the growing surface, which pins the step edges. Thus, the usual layer-by-layer growth obtained by MBE is not achieved under these conditions. New layers will start to nucleate and grow before the un-

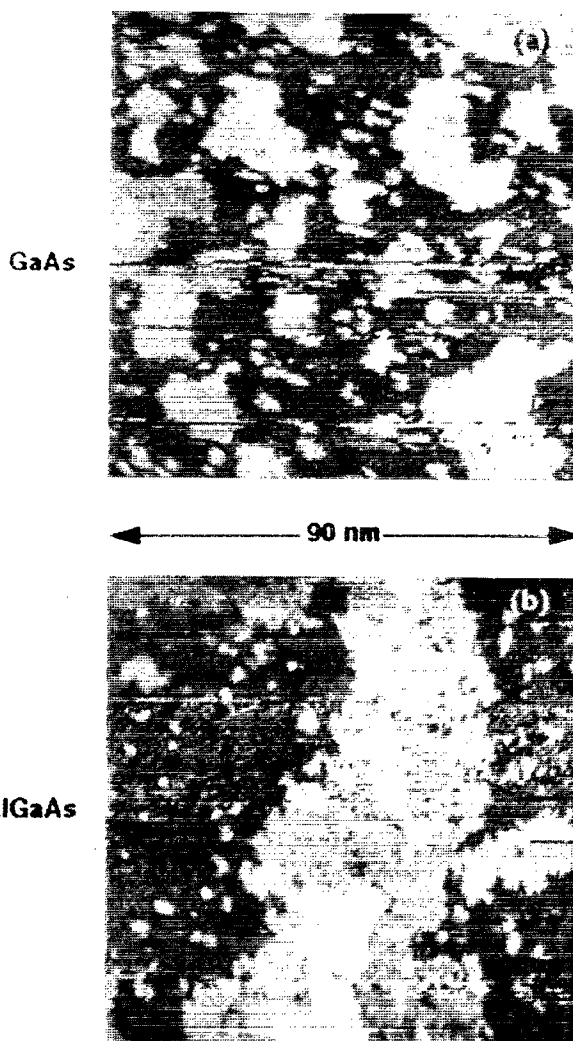


FIG. 8. UHV-STM images of growth-interrupted surfaces prepared under  $1 \times 10^{-10}$  Torr  $\text{O}_2$  conditions: (a) GaAs surface, (b)  $\text{Al}_{0.35}\text{Ga}_{0.65}\text{As}$  surface. Both images show a pseudosmooth or microrough island distribution (large islands with small islands on top).

derlying ones have been completed, leading to microrough growth.

Intermixing on (100) interfaces is inhibited in III–V systems because of the alternating composition of the (100) layers. When a layer of Ga is deposited onto an As-terminated substrate, for example, replacement of As atoms by the impinging Ga is impeded by the unfavorable Ga—Ga bonds that would be required. We performed molecular dynamics (MD) calculations in order to evaluate the magnitude of this effect, and to estimate the amount of interface mixing when  $\text{Al}_{0.35}\text{Ga}_{0.65}\text{As}$  is deposited on GaAs. MD simulations of MBE are performed at much higher deposition rates than those in experiments. The high rates are necessitated by the detailed nature of the simulations. The large number of calculations required limit the maximum feasible elapsed time of the simulations to several nanoseconds for systems of a few thousand particles. Simulations at different deposition rates show that the ma-

TABLE I. Estimated interface mixing for the binary pairs, GaAs/GaAs and AlAs/GaAs from molecular dynamics calculations.

Binary pair	Interface mixing (%)	$H_v$ (eV)	$T_s$ (°C)
GaAs/GaAs	29.7	0	900
GaAs/GaAs	16.9	0.8	900
GaAs/GaAs	1.2	3.0	900
AlAs/GaAs	9.4	3.0	900
AlAs/GaAs	7.7	3.0	550

jour component of interface mixing occurs as the deposited atom collides with the surface.<sup>9</sup> The latent heat of vaporization is released at this time, and provides energy to break the bonds and rearrange the material. The transient mobility due to the release of the latent heat is fully accounted for in the simulations, but the equilibrium diffusion is curtailed by the short time scale of deposition. Our approach was to compare systems simulated under identical conditions, but with different interaction energies between like and unlike species. In this way the importance of the unfavorable bonds between like species can be ascertained. The results for the absolute magnitude of the mixing at the interface, however, are not as reliable because of the short elapsed time of the simulation. Our model includes experimentally measured values of the bond strengths for both Ga—As and Al—As,<sup>10</sup> the individual covalent radii (As, Ga, Al),<sup>11</sup> and the thermal velocities of the impinging atoms onto the growing surface. The interaction potentials include pair and three-body terms and are based on the Stillinger–Weber potential for silicon.<sup>9</sup> Electronic effects on the interactions are not included.

The bonds between like species are not known to any degree of accuracy, and these bonds largely determine the energies of the anti-site defects. We chose to vary these bond energies in such a way as to give anti-site energies in the range of 0–3.0 eV. Typical published values of this defect vary from 2.5 to 4.5 eV.<sup>12</sup> In our model, the As anti-site has approximately the same energy as the Ga anti-site; a small difference results from the different covalent radii of the two species. Simulations were performed at 900 and 550 °C; the higher temperature was required in order to obtain measurable intermixing in some of the interfaces.

The model system consisted of a GaAs substrate containing 20 layers with 144 atoms in each. The atoms in the bottom layer were held fixed in the ideal bulk lattice sites. The next two layers were fully dynamic, but coupled to a constant temperature bath through random and dissipative forces. Periodic boundary conditions were applied to the sides of the computational cell. Two layers of GaAs or AlAs were deposited onto the GaAs substrate in order to evaluate the degree of intermixing.

Table I gives the results, where the amount of intermixing is measured by the number of deposited atoms that penetrated into the region of the substrate, and remained there after the growth of the films. (We found that deposition of films thicker than 2 monolayers did not significantly increase the intermixing at the interface.) Mixing ranged from almost 30% for no activation barrier to about

1% for  $H_v=3.0$  eV. This latter case reflects negligible mixing. We then investigated the effect of depositing an AlAs layer on GaAs as a function of substrate temperature with  $H_v=3.0$  eV. The results are listed in Table I. The small dependence with temperature indicates that interface mixing is most likely due to the  $\sim 0.4$  eV difference in bond strength between Al—As and Ga—As. In addition, no exchange was observed with the lower substrate bi-layer, only the top one. We estimate that there is about a 3% exchange of the Al and Ga atoms at the top SQW hetero-interface at 580 °C. Note that this is a high estimate of interface mixing, since we used a rather low  $H_v$  (3.0 eV) for the calculation.  $H_v$  is most likely closer to 4.0 eV, which would correspond to less than 1% mixing. This is in agreement with Guille *et al.*, who observed no segregation for either GaAs/AlAs or AlAs/GaAs interfaces using Auger spectroscopy.<sup>13</sup> We therefore believe that the surfaces imaged by UHV-STM are representative of the actual hetero-interfaces in our SQW samples.

We finally address the question of whether mixing processes between two semiconductors A and B, such as diffusion or segregation processes, can introduce microroughness. A semiconductor surface exhibiting microroughness will certainly result in a microrough interface. On the other hand, the surface may be very smooth (island size  $\gg 100$  Å), as demonstrated by our STM results. In order to clarify this question we introduce the interface-height function  $h(x,y)$ , where the cartesian coordinates  $x$  and  $y$  are in the plane of the interface. For simplicity we restrict ourselves to one direction,  $x$ , and the interface-height function along the  $x$  direction  $h(x)$ . The interface roughness spectrum is then the convolution of the interface-height function,

$$H(k) = \frac{1}{\sqrt{2\pi}} \int_{-\infty}^{\infty} h(x)h(x-x^*)dx^*,$$

where  $H(k)$  is the (power) spectrum of the interface function  $h(x)$  and  $k=2\pi/x$ . If, for example,  $h(x)$  is strictly periodic with a step height of one monolayer and a period of  $x_p=1000$  Å (island size of 500 Å), the roughness spectrum  $H(k)$  will have a  $\delta$  function at  $k=2\pi/x_p$ . It is important to visualize that any random changes in  $h(x)$ , caused by the well-known processes of diffusion or segregation will not introduce any additional roughness at  $k \neq 0$ . Such diffusion and segregation processes are due to random atomic hops, which cannot introduce a roughness component of, e.g., 50 Å. We therefore emphasize that interface roughness is a result of surface roughness which, in turn, can be assessed by STM.

In conclusion, we report on the effect of background vacuum conditions during the growth of growth-interrupted  $\text{Al}_{0.35}\text{Ga}_{0.65}\text{As}/\text{GaAs}/\text{Al}_{0.35}\text{Ga}_{0.65}\text{As}$  SQW samples on the PL emission characteristics. Constant PL emission energies were obtained, both across each sample and from sample to sample for a given well geometry, when grown under UHV conditions. However, when SQW samples were grown in the presence of  $10^{-10}$  Torr  $\text{O}_2$ , emission energies varied both across each sample, and from sample to sample for a given well geometry. These results are supported by UHV-STM images of growth-interrupted

GaAs and  $\text{Al}_{0.35}\text{Ga}_{0.65}\text{As}$  surfaces, which were prepared under identical conditions as the SQWs. The STM images show that islands, which are larger than the exciton diameter, are obtained for both GaAs and  $\text{Al}_{0.35}\text{Ga}_{0.65}\text{As}$  surfaces when the structures are grown under UHV conditions. However, a pseudosmooth or microrough surface is obtained when structures are grown in the presence of  $10^{-10}$  Torr  $\text{O}_2$ . These results show that interface roughness is extremely sensitive to background  $\text{O}_2$ . We believe that the UHV-STM images of the surfaces are representative of the actual interfaces obtained in the SQW samples, since molecular dynamics calculations show negligible interface mixing.

<sup>1</sup>D. Gammon, B. V. Shanabrook, and D. S. Katzer, *Appl. Phys. Lett.* **57**, 2710 (1990).

<sup>2</sup>T. R. Block, D. P. Neikirk, and B. G. Streetman, *J. Vac. Sci. Technol. B* **10**, 832 (1992).

<sup>3</sup>R. F. Kopf, E. F. Schubert, T. D. Harris, and R. S. Becker, *Appl. Phys. Lett.* **58**, 631 (1991).

<sup>4</sup>C. A. Warwick and R. F. Kopf, *Appl. Phys. Lett.* **60**, 386 (1992).

<sup>5</sup>T. Noda, M. Tanaka, and H. Sakaki, *J. Cryst. Growth* **111**, 348 (1991).

<sup>6</sup>P. Ils, J. Kraus, G. Schaack, G. Weimann, and W. Schlapp, *J. Appl. Phys.* **70**, 5587 (1991).

<sup>7</sup>J. H. Neave, B. A. Joyce, P. J. Dobson, and N. Norton, *Appl. Phys. A* **31**, 1 (1983).

<sup>8</sup>A. Madhukar, T. C. Lee, M. Y. Chen, J. Y. Kim, S. V. Ghaisas, and P. G. Newman, *Appl. Phys. Lett.* **46**, 1148 (1985).

<sup>9</sup>*Handbook of Crystal Growth*, edited by D. T. J. Hurle (North-Holland, Amsterdam, 1992).

<sup>10</sup>*The Technology and Physics of Molecular Beam Epitaxy*, edited by E. H. C. Parker (Plenum, New York, 1985), p. 592.

<sup>11</sup>Sargent-Welch Scientific Company, *Table of Periodic Properties of the Elements*, 1968.

<sup>12</sup>L. C. Kimerling (private communication).

<sup>13</sup>C. Guille, F. Houzay, J. M. Moison, and F. Barthe, in *Institute of Physics Conference Series No. 91*, edited by A. Christou and H. S. Rupprecht (Institute of Physics, Bristol, UK, 1988), p. 327.